Electrostatic Tuning of a Micro-Ring Gyroscope

B.J.Gallacher*, J. Hedley*, J. S. Burdess*, A. J. Harris*, A. Rickard** and D. King**

*1Institute for Nanoscale Science & Technology, Newcastle University,U.K., b.j.gallacher@ncl.ac.uk
**QinetiQ (Malvern), St Andrews Rd, Malvern, Worcs, U.K.

ABSTRACT

This paper describes a procedure for identifying and correcting anisoinertia and anisoelasticity present in a micro-ring gyroscope. The major disadvantages of popular tuning methods such as mass trimming using laser ablation or focussed ion beam is that it can only be employed prior to packaging. Therefore tuning to correct for environmental or structural changes during operation is not possible. However, electrostatic tuning may be implemented on-chip during operation thus enabling active tuning. Furthermore, mass trimming procedures introduce a degree of damage to the structure, which may reduce the intrinsic high quality factor desirable in the ring gyroscope.

Keywords: tuning, electrostatic, gyroscope, ring

1 INTRODUCTION

The isotropic inertial and elastic properties of a perfectly formed axisymmetric ring ensure that the flexural modes of vibration exist in degenerate pairs. Thus the natural frequencies of the modes within each pair are identical and their orientation is indeterminate. This "tuned" phenomenon may be utilised in order to improve the performance of ring gyroscopes. Any structural imperfection introduced in the ring or its suspension during fabrication or operation will result in anisotropic inertial and elastic properties [1,2]. This is manifested as a frequency split between the otherwise "tuned" natural frequencies, which reduces the sensitivity of the gyroscope to rates of rotation. In addition, the modes of vibration are coupled both statically and inertially. As the ring gyroscope utilises Coriolis coupling between the modes of vibration in order to sense rate of rotation, the anisoinertia and anisoelasticity must be minimised in order to prevent spurious measurements. Further, as the quality factor of typical ring gyroscope may be in excess of 10000, precise tuning of the modes is essential in order to take full advantage of the amplification possible through matching the mode frequencies. With such tuning control the overall performance of the ring gyroscope will be greatly improved and may lead to inertial grade MEMS gyroscopes.

2 DYNAMICS OF THE IMPERFECT RING

Figure (1) shows a schematic of the QinetiQ ring gyroscope of ring of radius a, width b and thickness d and the electrode displaced radially from the ring by a distance h_o. The dynamics of the ring are expressed with respect to an axis X passing through the ring centre O and the midpoint of an electrode.

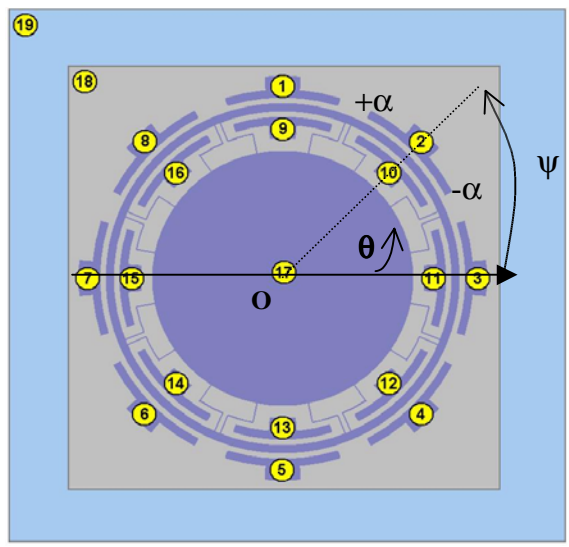

Figure (1) Schematic of Gyroscope

The radial displacement u of a point on the centre line of the ring may be expressed in terms of the undamped, unforced flexural modes of an unsupported ring by

$$u = q_1 \cos n\theta + q_2 \sin n\theta. \quad (1)$$

The electrical energy stored in the capacitor, formed between the ring (assumed to be held at earth potential) and the drive electrode, biased with a voltage V is given by

$$E_E = \frac{\varepsilon_o a d}{2h_o} V_i^2 \int_{\psi-\alpha}^{\psi+\alpha} \left[1 + \frac{u}{h_o} + \left(\frac{u}{h_o}\right)^2 + \left(\frac{u}{h_o}\right)^3 + \cdots \right] d\theta. \quad (2)$$

It is assumed that the air-gap h_o, is small with respect to the ring radius and so the ring and the electrode form a parallel plate capacitor. As the radial displacement of the ring is assumed to be small compared to the nominal air gap separation, terms of order greater than $(u/h_o)^3$ may be ignored. Fringing effects between adjacent electrodes are neglected. The generalised stiffness matrix and forcing vector for the arbitrary drive electrode may be obtained from substituting in the expression for the radial displacement given by equation (1) into equation (2) and by determining dE_E/dq_i and d^2E_E/dq_i^2 for i=1..2.

Consider the general case where driving is performed by activating the $\overline{Z}$ electrodes positioned at the antinodal postions of the $\sin n\theta$ mode and tuning is performed using a set consisting of t electrodes. The equation of motion for the in-plane flexural modes of order n may be written in the form

$$\begin{bmatrix} 1+\varepsilon_1 & \varepsilon_2 \\ \varepsilon_2 & 1-\varepsilon_1 \end{bmatrix}\begin{bmatrix} \ddot{q}_1 \\ \ddot{q}_2 \end{bmatrix} + \frac{1}{m_o}\left\{ k_o \begin{bmatrix} 1+\mu_1 & \mu_2 \\ \mu_2 & 1-\mu_1 \end{bmatrix} - \sum_{j=1}^{t} [K]_j \right\}\begin{bmatrix} q_1 \\ q_2 \end{bmatrix} = \frac{1}{m_o}\overline{Z}\beta V_{\overline{z}}^2 \begin{bmatrix} 0 \\ 1 \end{bmatrix} \quad (3)$$

where $\beta = \dfrac{\varepsilon_o a d}{h_o^2}\dfrac{1}{n}\sin(n\alpha)$

and $\varepsilon_1, \varepsilon_2, \mu_1$ and μ_2 represent perturbations in the generalised mass and stiffness values, m_o and k_o of the ideal ring. In the perfectly axisymmetric case the natural frequencies of both modes corresponding to generalised coordintes q_1 and q_2 are equal thus $\omega_1=\omega_2$. Damping is assumed small and has been neglected. The electrostatic stiffness matrix from the tuning electrodes may be expressed in the form

$$\sum_{j=1}^{t}[K]_j = \sum_{l}^{L}[K_c]_l + \sum_{m}^{M}[K_s]_m = Lk_o\lambda_c\begin{bmatrix} 1 & 0 \\ 0 & \sigma \end{bmatrix} + Mk_o\lambda_s\begin{bmatrix} \sigma & 0 \\ 0 & 1 \end{bmatrix} \quad (4)$$

where

$$\sigma = \frac{\left(2\alpha - \frac{1}{n}\sin 2n\alpha\right)}{\left(2\alpha + \frac{1}{n}\sin 2n\alpha\right)}, \quad \sigma << 1,$$

and

$$k_o\lambda_{c,s} = \left(2\alpha + \frac{1}{n}.\sin 2n\alpha\right)\frac{\varepsilon_o a d}{2h_o^3}U_{c,s}^2$$

The cyclic arrangement of tuning electrodes has been separated into two distinct sets with each set consisting of a maximum of $2n$ electrodes. The parameters L and M are the number of tuning electrodes employed. The two sets of electrodes corresponding to stiffness matrix K_c and K_s may be employed to reduce the natural frequencies of the $\cos(n\theta)$ and $\sin(n\theta)$ modes respectively. Which set of electrodes is used depends on which mode has the higher natural frequency. For example, suppose $\omega_1>\omega_2$, then reduction of the natural frequencies of the $\cos(n\theta)$ mode is achieved by employing the set corresponding to stiffness matrix K_c. Similarly, if $\omega_2>\omega_1$ then reduction of the natural frequencies of the $\sin(n\theta)$ mode is achieved by employing the set corresponding to stiffness matrix K_s. However, it will be shown later that if any coupling between the $\cos(n\theta)$ and $\sin(n\theta)$ modes is present then it will be impossible to completely eliminate the frequency split such that $\omega_1=\omega_2$. Removal of the coupling between the modes is not possible with this electrode configuration for the n=2 case.

The external force and thus the response are assumed to be harmonic with frequency ω. Therefore,

$$V_1^2 = V_{01}^2 e^{i\omega t} \text{ and } q_1 = q_{01}e^{i(\omega t-\delta)}, \; q_2 = q_{02}e^{i\omega t} \quad (5)$$

where δ=0,π and represents the phase angle between the responses. Assuming excitation occurs near resonance then

$$\omega^2 = p^2(1+\eta) \text{ where } \eta << 1 \quad (6)$$

and p is the natural frequency of the undamped perfect ring. By making use of equations (4), (5) and (6), equation (3) may be written in the form

$$[Y]\begin{bmatrix} q_{01}e^{-i\delta} \\ q_{02} \end{bmatrix} = \frac{1}{m_o}\overline{Z}\beta V_{\overline{z}}^2\begin{bmatrix} 0 \\ 1 \end{bmatrix}$$

$$\text{where } [Y] = p^2\begin{bmatrix} A+B-\eta & C \\ C & A-B-\eta \end{bmatrix}. \quad (7)$$

The terms A, B and C defined as

$$A = -(1+\sigma)[L\lambda_c + M\lambda_s]$$

$$B = f - \frac{L\lambda_c}{2}(1-\sigma) - \frac{M\lambda_s}{2}(1-\sigma)$$

$$C = g$$

where

$$f = \varepsilon_1 - \mu_1 \text{ and } g = \varepsilon_2 - \mu_2.$$

The natural frequencies of the imperfect ring may be obtained from the requirement that $|Y=0|$, which yields the expression

$$\eta = A \pm \sqrt{B^2 + C^2}. \quad (8)$$

The frequency split between the modes is therefore given by

$$|\omega_1 - \omega_2| = \Delta\omega \approx p\sqrt{B^2 + C^2}. \quad (9)$$

The conditions B=0 and C=0 are necessary for identical natural frequencies and yield

$$f = \frac{1}{2} L\lambda_c(1-\sigma) - \frac{1}{2} M\lambda_s(1-\sigma) \tag{10}$$

Clearly for this electrode configuration the coupling between the modes determined by g cannot be altered and thus $C \neq 0$. Appropriate values for λ_c, λ_s, must to chosen in order to remove the direct imperfection parameters f.

3 DETERMINING THE MIS-TUNING AND IMPERFECTION PARAMETERS

When λ_c=λ_s=0, equation (8) reduces to $\eta = \pm\sqrt{f^2 + g^2}$. Therefore the damped natural frequencies of the imperfect ring are

$$\omega_1 \approx p\left(1 \pm \frac{1}{2}\eta_c\right) \tag{11}$$

$$\omega_2 \approx p\left(1 \mp \frac{1}{2}\eta_c\right) \tag{12}$$

where $\eta_c = \sqrt{f^2 + g^2}$. (13)

In addition, an expression for η_c in terms of the undamped natural frequencies may be obtained using equations (11) and (12). Thus

$$\eta_c = 2\left|\frac{(\omega_1 - \omega_2)}{\omega_1 + \omega_2}\right|. \tag{14}$$

To determine f and g, recall the equation of motion described by equation (7). Multiplying both sides of equation (7) by the inverse of the matrix Y, when λ_c=λ_s= 0 yields

$$\begin{bmatrix} q_{01}e^{-i\delta} \\ q_{02} \end{bmatrix} = \frac{\beta \bar{Z} V_{\bar{z}}^2 p^2}{m_o|Y|} \begin{bmatrix} -(f+\eta) & -g \\ -g & (f-\eta) \end{bmatrix} \begin{bmatrix} 0 \\ \pm 1 \end{bmatrix} \tag{15}$$

where

$$|Y| = \eta^2 - f^2 - g^2. \tag{16}$$

From equation (16), it is clear that identical values of $|Y|$ are obtained for $\eta = \pm\eta_c$. The ratio of the amplitudes of the modes when driven at their respective natural frequencies corresponding to $\eta = \pm\eta_c$ is given by

$$r = \frac{q_{01}(\pm\eta_c)}{q_{02}(\mp\eta_c)} = \frac{-g}{f \pm \eta_c} e^{i\delta}. \tag{17}$$

The phase angle δ between the modes may be determined from Nyquist plots of displacement or velocity frequency response. The substitution of g from equation (17), into the expression for η_c given by equation (13) yields a quadratic equation in f of which the permissible roots are

$$f = \pm\eta_c\left[\frac{1-r^2}{1+r^2}\right]. \tag{18}$$

Equations (17) and (18) show that the imperfection parameters f and g are now expressed in terms of measurable quantities r, η_c and δ. The signs of f and g are determined from r and δ.

For $r = \frac{q_{01}(\eta_c)}{q_{02}(-\eta_c)}$, $f > 0 \Leftrightarrow r < 1$ and $g > 0 \Leftrightarrow \delta = \pi$. (19)

For $r = \frac{q_{01}(-\eta_c)}{q_{02}(+\eta_c)}$, $f > 0 \Leftrightarrow r > 1$ and $g > 0 \Leftrightarrow \delta = 0$. (20)

Clearly from equation (18), f=0 when r=1.

4 CORRECTION OF ANISOINERTIA AND ANISOELASTICITY

The frequency split due to the imperfection parameter f may be removed using the set of electrodes corresponding to stiffness matrix K_c or K_s. The decision as to which set of electrodes are employed is determined by the sign of f. The sign of f may be determined from equations (19) and (20). From equation (10) the condition B=0 is met when

$$\lambda_c = \frac{2f}{L(1-\sigma)} \quad \text{if } f > 0 \tag{21}$$

$$\lambda_s = \frac{-2f}{M(1-\sigma)} \quad \text{if } f < 0. \tag{22}$$

Thus, the voltages required to be applied to the two tuning electrode sets to remove the imperfection due to f are given by

$$U_c^2 = \frac{1}{\left(2\alpha + \frac{1}{n}.\sin 2n\alpha\right)} X\omega_{1,2}^2 m_o \lambda_c \text{ and } U_s^2 = 0 \text{ for } f > 0 \tag{23}$$

$$U_s^2 = \frac{1}{\left(2\alpha + \frac{1}{n}.\sin 2n\alpha\right)} X\omega_{1,2}^2 m_o \lambda_s \text{ and } U_c^2 = 0 \text{ for } f < 0. \tag{24}$$

where $\omega_{1,2}$ corresponds to either of the undamped natural frequencies ω_1 and ω_2 of the imperfect ring.

5 PRACTICAL DEMONSTRATION

The drive and sense circuitry is shown in figure (2). Mode (1) and mode (2) correspond to the sin($n\theta$) and cos($n\theta$) modes, respectively. A bias of 30 V was placed on the ring; the silicon substrate, chip and the two unused sense electrodes were also set to this voltage. In order to investigate the electrostatic tuning process over a larger range, artificial mis-tuning was introduced by applying a -60 V bias (with respect to the ring) to the set of tuning electrodes corresponding to the sin($n\theta$) mode. For this device ω_1>ω_2. Thus a variable voltage supply was

connected to the set of tuning electrodes corresponding to the cos($n\theta$) mode. In this case four tuning electrode were used to adjust the direct terms so L=4. Table (1) shows describes the device dimensions.

a (mm)	2.05
b (µm)	100
d (µm)	100
α (deg)	14.25
h_o (µm)	4.7+/-0.25

Table 1: Device dimensions

The sin($n\theta$) mode of the gyroscope was driven with 0.25 V a.c with a 25 V d.c. component. Two drive electrodes were employed thus $\overline{Z} = 2$. The current detected by the sense electrodes of each mode was converted to a voltage and fed into a HP-3562 dynamic signal analyser together with the a.c. drive signal. The remaining drive and sense electrodes were held at the same potential as the ring. All dynamic measurements were obtained at a pressure of 0.02 mbar.

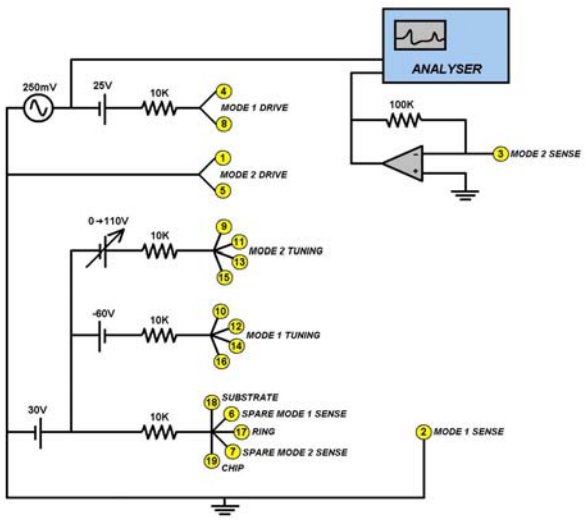

Figure (2) Experimental set-up

5.1 Tuning voltage

Table (2) shows the measured values of r, η_c, δ and. also the imperfection parameters f and g determined from r, η_c and δ by equations (17) and (18). The electrode configuration of the device does not permit adjustment of the coupling between the cos($n\theta$) and sin($n\theta$) modes for the case where n=2. Therefore the imperfection parameter g will remain constant throughout the tuning procedure and will ultimately determine the minimum frequency split. For this device f >0 and the value of the voltage U_c required to eliminate f is described by equation (23). The tuning voltage U_c corresponding to the electrode gap size of 4.7+/-0.25 µm has the value of 59.4 +/- 4.9 V.

parameter	value
η_c	0.0076
r	0.1025
δ	π
f	0.0074
g	0.0015

Table 2:Imperfection parameters

5.2 Tuning cuves

Figure (3) illustrates the theoretical and experimental tuning curves obtained using equations (9) and (23) with M=0. Two theoretical curves corresponding to the +/- 0.25 µm tolerance on the nominal value of the electrode gap have been drawn to create the band shown in the figure.

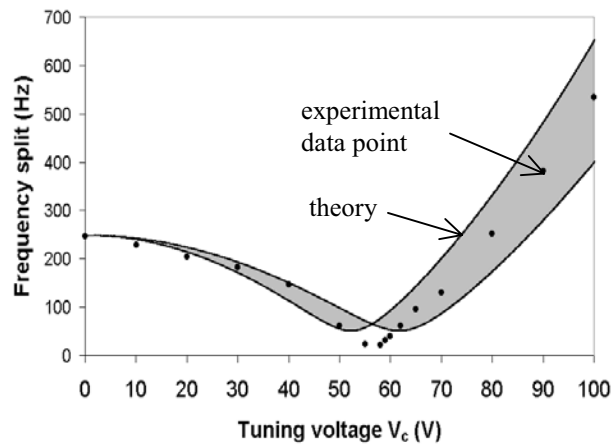

Figure (3) Frequency split versus voltage with coupling between modes present

6 CONCLUSION

The predicted tuning voltage to remove the direct imperfections was found theoretically to be 59.4 +/- 4.9 V. Experimentally the voltage at which the frequency split was a minimum occured at a voltage of 58 V. Therefore there is agreement between the theoretical model and experiment. The cross-coupling between the modes is not altered for the electrode arrangement considered when n=2. Additional electrodes would have to be used in order to permit adjustment of the cross-coupling and hence completely eliminate the frequency split between the modes.

REFERENCES

1. B.J. Gallacher et al. "Multimodal tuning of a vibrating ring using laser ablation" *Journal of Mechanical Engineering Science*, Part C, vol.217, p557-576.

2. C. Painter and A. Shkel. "Identification of anisoelasticity for electrostatic trimming of rate integrating gyroscopes", *2002 SPIE Annual International Symposium on Smart Structures and Materials*, San Diego, CA, March 2002.